NIPPON STEEL TECHNICAL REPORT No. 95 January 2007

UDC 621 . 791 . 75 : 681 . 3

Process Modeling of Short-Circuiting GMA Welding and Its Application to Arc Sensor Control

Shinji KODAMA*1 Yasutomo ICHIYAMA*1
Yasuyuki IKUNO*2 Norimitsu BABA*2

Abstract

The mathematical model of gas metal arc (GMA) welding, focusing on short-circuiting transfer, is developed. First, a model of short arc welding is proposed, based on a previous reported model of spray arc welding. Then, the proposed model applied to the high speed oscillating GMA process, and the short-circuiting dynamics is investigated. Numerical calculation result revealed that short-circuiting regularly occurs at both oscillating edges at oscillating frequencies close to half the rate of short-circuiting under non-oscillating condition. The finding indicates that the arc sensor properties improved by setting the oscillating frequency to this value.

1. Introduction

In gas metal arc (GMA) welding, the welding wire itself serves as the electrode. Since the electrode wire is melted by the arc heat and transferred to a molten pool in the form of hot droplets, its melting characteristics influence the current and voltage characteristics in the arc welding system.

Various models for arc welding systems have been developed, mainly to analyze the wire-melting phenomenon. Lesnewich[1] and Halmoy[2] derived a wire-melting characteristic formula based on the spray transfer conditions under which the mode of hot-droplet transfer stabilizes. Maruo et al.[3] derived the optimum current conditions by applying this to pulsed arc welding. Ushio et al.[4, 5] analyzed the dynamic melting characteristics of wire and built a model for the arc welding system taking into account the power supply responsiveness (inductance, etc.) and the change in torch height due to its weaving in the groove. This model, in particular, has been applied to analyze the performance of arc sensors and has helped establish the foundations for excellent arc sensor systems, such as the high speed rotating arc welding process[6].

On the other hand, in GMA welding, not only spray transfer conditions are widely employed, but also short-circuiting arc conditions with a relatively small current. Short-circuiting arc welding is the mainstream in high-speed welding of thin sheets or overhead position welding of line pipes. However, because of the complicated process in which short-circuiting and arc generation are repeated intermittently, there are few papers on short-circuiting arc welding[7]. Besides, in short-circuiting arc welding, it is difficult to distinguish between the changes in welding current/voltage due to short-circuiting and those due to a change in positional relationship between the groove and electrode wire. Under this condition, there is the concern that the accuracy of seam tracking of arc sensors would decline.

Therefore, with the aim of better understanding the welding phenomena, an attempt was made to develop a model for short arc welding on the basis of a previous reported model for spray arc welding. In addition, by applying the newly developed model, an analysis was conducted on the short-circuit behavior in the high-frequency oscillating GMA process to enable a discussion of the guidelines on optimization of arc sensor properties. The variables used for the model are shown at the end of this paper.

2. Modeling of Arc Welding System

2.1 Spray transfer model

Concerning the spray transfer conditions, many study results have been reported. In this paper, reference is made to the mathematical model[4] developed by Ushio et al. taking into account the dynamic

*1 Steel Research Laboratories

*2 Nippon Steel Engineering Co., Ltd.

characteristics of wire melting. **Fig. 1** shows the equivalent electrical circuit for typical GMA welding employing a power supply having constant voltage characteristics, and equations (1) through (9) represent its mathematical model.

Equations (1) and (2) are the relational expressions of torch height L_t and torch voltage U_t. They are expressed by the sum of the wire extension component and arc component.

$$L_t = L_a + L_e \quad (1)$$

$$U_t = U_a + U_e \quad (2)$$

Arc voltage U_a is expressed by the following relational expression of welding current I and arc length L_a.

$$U_a = U_{a0} + R_a I + E_a L_a \quad (3)$$

The following equation (4) expresses voltage drop U_e at the wire extension, and the value of Ue can be calculated from wire resistance R_e during current conduction expressed by equation (5).

$$U_e = R_e I \quad (4)$$

The value of R_e is obtained as an integrated value along the wire length by using the Joule heating weight J_z at position Z on the wire defined by equation (6) (see Fig. 1) and relational expression $r(J_z)$ of J_z and resistance value.

$$R_e = \int_0^{L_e} r(J_z)\, dz \quad (5)$$

$$J_z = \int_{t - z/V_f}^{t} I^2(\tau)\, d\tau \quad (6)$$

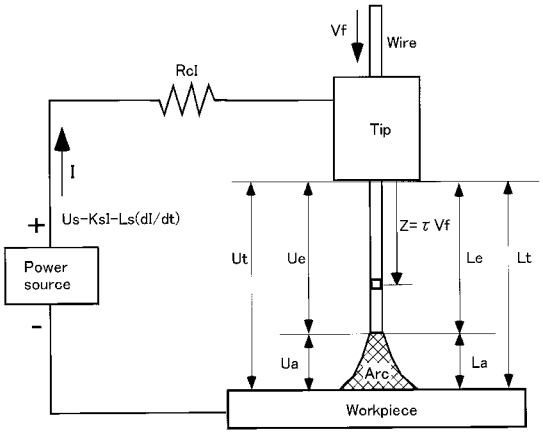

Fig. 1 Equivalent electrical circuit for GMA welding (Ref.4)

Equation (7) is the relational expression of the equivalent electrical circuit for GMA welding. In the left-hand side of the equation, U_s, K_s and L_s denote no-load voltage, internal resistance and power supply inductance, respectively. $R_c I$ and U_t in the right-hand side represent power cable voltage drop and torch voltage, respectively.

$$U_s - K_s I - L_s \left(\frac{dI}{dt}\right) = R_c I + U_t \quad (7)$$

Equation (8) represents the amount of variation of wire extension length L_e that is expressed as the difference between wire feeding speed V_f and wire melting speed V_m. As shown in equation (9), the value of V_m is obtained as the function of welding current I and Joule heating weight J_{Le} at the tip of the wire extension[4]. In equation (9), A denotes the coefficient of arc heating in wire melting, and B denotes the coefficient of Joule heating.

$$\frac{dL_e}{dt} = V_f - V_m \quad (8)$$

$$V_m = \frac{AI}{1 - BJ_{Le}} \quad (9)$$

2.2 Short-circuiting transfer model

An attempt was made to develop a short-circuiting arc model using the spray arc model. In the spray arc model, it was assumed that hot droplets would be continuously transferred from the wire tip to the base metal at melting speed V_m. In the case of a short-circuiting arc, however, it is considered that each hot droplet grows at the wire tip during arc generation, thereby shortening the arc length and causing the droplet to be transferred to the base metal in the short-circuited state. Therefore, a discussion ensued with regard to the short-circuiting arc in two different periods–the open-arc period and the short-circuiting period–as shown in **Fig. 2**. In addition, since it was necessary to consider the hot droplet at the wire tip, wire extension length L_e was divided into unmelted wire length L_{es} and droplet length L_{em}.

$$L_e = L_{es} + L_{em} \quad (10)$$

Equations (11) through (16) represent the calculation model for the open-arc period. It was assumed that all the molten metal would turn into droplets at the tip of the wire. The molten pool profile (depression, etc.) was left out of consideration. Equation (11) expresses the initial condition of droplet length. On the assumption that each droplet would be completely transferred to the base metal during the short-circuiting period, droplet length L_{em} at the instant, t_{ia}, at which an arc is generated was assumed to be zero.

$$L_{em}(t_{ia}) = 0 \quad (11)$$

The condition for arc generation is given by the following equa-

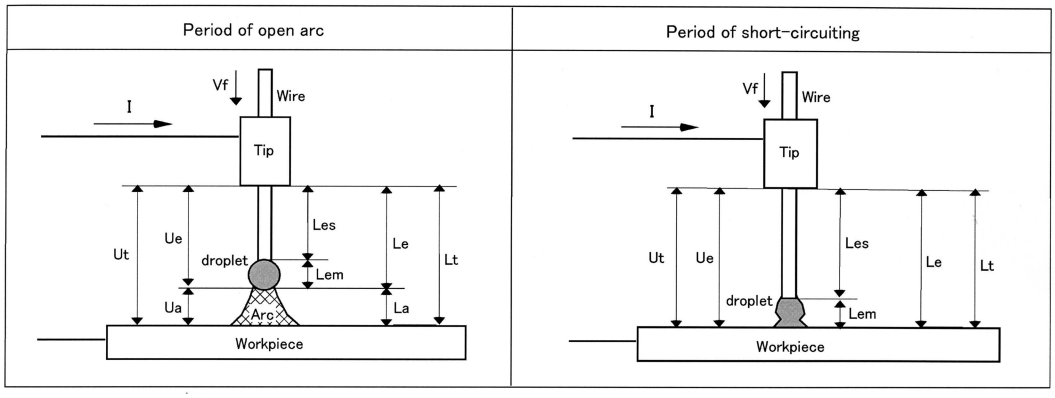

Fig. 2 Schematic representation of short circuiting transfer mode

tion. When L_e becomes greater than torch height L_t, the short-circuiting period begins.

$$L_t \geq L_e \tag{12}$$

As is evident from equation (10), L_e is determined by the relative rates of change of L_{es} and L_{em}. Thus,

$$\frac{dL_e}{dt} = \frac{dL_{es}}{dt} + \frac{dL_{em}}{dt} \tag{13}$$

L_{es} is given by the following equation. To obtain V_m, equation (9) applicable in the open-arc period was directly applied.

$$\frac{dL_{es}}{dt} = V_f - V_m \tag{14}$$

Droplet length L_{em} at the wire tip was defined by the following equations (15) and (16). Namely, L_{em} was decided by multiplying R_m, the value of which was obtained by assuming that the tip of a wire having cross-section area S would turn into a spherical droplet having radius R_m when melted at melting speed V_m, by constant α which represents the droplet shape.

$$\frac{4}{3}\pi R_m^3 = S\int_{t_{ia}}^{t} V_m(\tau)\, d\tau \tag{15}$$

$$L_{em} = \alpha R_m \tag{16}$$

The droplet shape depends on the shielding gas, welding position, etc. When an 80% Ar + 20% CO_2 shielding gas, which readily tends to cause a spray transfer, or downward welding position is adopted, it is considered that the droplet will take on an elongated form. In this paper, therefore, it is assumed that $\alpha = 3$ and that the droplet length is 1.5 times the spherical droplet length assumed in equation (15).

Equations (17) ~ (19) represent the calculation model for the short-circuiting period. When arc length L_a is assumed to be zero, droplet length L_{em} is determined by the rate of change of the torch height, the wire feeding speed and the wire melting speed.

$$\frac{dL_{em}}{dt} = \frac{dL_t}{dt} - V_f + V_m \tag{17}$$

During short-circuiting, the welding current increases and droplet necking is enhanced. It is considered, therefore, that the Joule heating of the wire extension governs the melting of the wire[8]. Therefore, the value of V_m was attained during short-circuiting while taking into account only the influence of Joule heating as shown in equation (18).

$$V_m = B_1 R_e I^2 \tag{18}$$

Droplet necking plays an important part in the short-circuiting transfer process. Because of this, the influences of short-circuit current and droplet size on the droplet necking formation have been studied[9]. On the other hand, droplet length L_{em} when the torch is oscillating is influenced not only by the droplet growth (increase in droplet weight) due to Joule heating, but also by the change in torch height due to torch oscillation. It is considered, therefore, that when the torch approaches either of its oscillation ends, L_{em} shortens due to a decrease in torch height and necking of the droplet is restrained. On the other hand, as the torch is distanced from the oscillation end, L_{em} increases, enhancing the droplet necking and shortening the short-circuiting transfer time.

Therefore, as a term of promotion of short-circuiting transfer, the square of welding current was used and L_{em} as shown in equation (19). It was assumed that the short-circuiting transfer would end when the integrated value of their products in the period from the time, t_{is}, when the short-circuiting begins reaches the prescribed value β.

$$\int_{t_{is}}^{t} I(\tau)^2 L_{em}(\tau)\, d\tau \leq \beta \tag{19}$$

The measured short-circuiting time was approximately 3 ms. In order to reproduce this short-circuiting time, the value of β was fixed at 200.

3. Model-based Analysis and Discussion on Arc Sensor Performance

Using the short-circuiting welding model described above, a study was conducted the condition for occurrence of short-circuiting due to oscillations of the torch by means of a numerical analysis applying difference calculus. The unit time used for the calculations was 0.5 ms and the calculation results obtained in 1 to 3 s were evaluated. It has been confirmed that the results of calculations in 1 s or more reach a stationary state. The parameters for arc characteristics and wire melting characteristics were decided based on the values given in reference material[4-7].

As the conditions for the short-circuiting arc, V_m = 83.3 mm/s, U_s = 22.6 V and torch height L_t = 18 mm at the center of oscillation were used. Average welding current and average torch voltage were assumed to be 190 A and 17.9 V, respectively, and short-circuiting frequency, N_{so}, without torch oscillations was assumed to be 80 times/s.

Fig. 3 shows the calculated welding currents and torch voltage waveforms without oscillation of the torch. At the same time that short-circuiting starts, the voltage begins to drop sharply and the current begins increasing. The current continues increasing for the short-circuiting period, that is, the period for which the condition of equation (19) is met. The rate at which the current increases depends on the inductance of the welding power supply. The smaller the inductance, the higher is the rate of current increase and hence, the shorter becomes the short-circuiting period. It should be noted that the amount of increase in voltage during the short-circuiting period is somewhat smaller than in the actual welding phenomenon. This is because the increase in wire resistance due to necking formation is excluded from consideration. When the short-circuiting period ends, an arc occurs, causing the voltage to increase sharply and the current to start decreasing slowly. During the open arc period, the voltage drops slowly as the arc length decreases due to growth of the droplet.

As described above, by using the short-circuiting welding model, it is possible to reproduce the dynamic welding phenomenon within

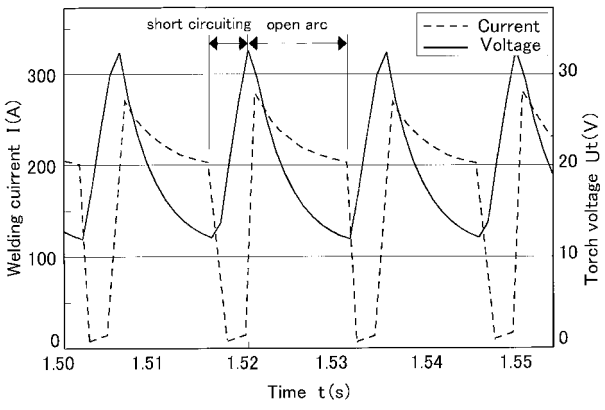

Fig. 3 Simulation result of torch voltage and welding current

the short-circuiting period.

3.1 Short-circuiting dynamics in high-frequency oscillating GMA process

Taking into consideration the experimental results, an analysis was conducted on the short-circuiting dynamics under oscillations of the torch in the groove. **Fig. 4** shows the relationship between oscillating torch position X in the groove and torch height L_t. The change of L_t was decided based on the assumption that the arc would spread about 3 mm for a groove with a root gap of 5 mm. Namely, it was assumed that a mutual interference between the arc and groove wall would occur when $|X| > 1.0$ mm, causing L_t to decrease by 1.5 mm at each oscillation end ($|X| = 1.5$ mm). The oscillating torch position was expressed by the simple harmonic motion of oscillation width W and oscillation frequency f as shown in equation (20).

$$X = (W / 2) \sin (2\pi ft) \qquad (20)$$

Fig. 5 shows the measured and calculated torch voltage waveforms at torch oscillation frequencies of 10, 40 and 50 Hz. In the diagrams showing the measured waveforms, timings (L, R) at both ends of the torch oscillations are indicated on the upper horizontal axis. It can be seen that both the measured and calculated waveforms show a similar trend. When f = 10 Hz, short-circuiting occurs several times at the time that the torch approaches either of its oscillation ends, but the short-circuiting position is not limited to the oscillation end. When f = 40 Hz, short-circuiting occurs regularly at either oscillation end. When f = 50 Hz, the short-circuiting phenomenon does not follow the torch oscillation anymore, although the position at which short-circuiting occurs is limited to either oscillation end.

Fig. 6 shows the relationship between oscillation frequency and the rate of short-circuiting. It can be seen that the calculation results agree well with the experimental results. Namely, when f is in the range 30 to 45 Hz, the short-circuiting frequency N_s is twice the value of f. Each time the torch oscillates in the groove, the wire approaches the left and right groove walls once. It is considered, therefore, that when the oscillation frequency nears half of the short-circuiting frequency without torch oscillations, the droplet is regularly transferred at the left and right groove walls. When f < 30 Hz, the value of N_s is

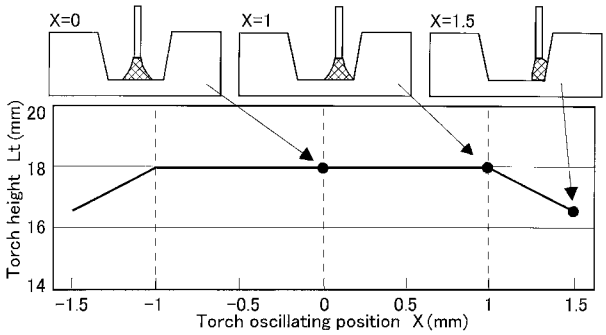

Fig. 4 Torch height variation during torch oscillation in groove

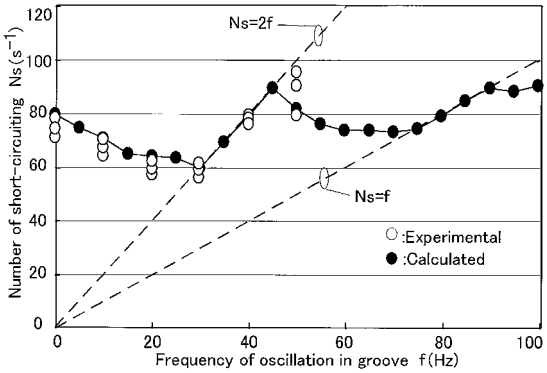

Fig. 6 Relationship between torch oscillating frequency and number of short-circuiting

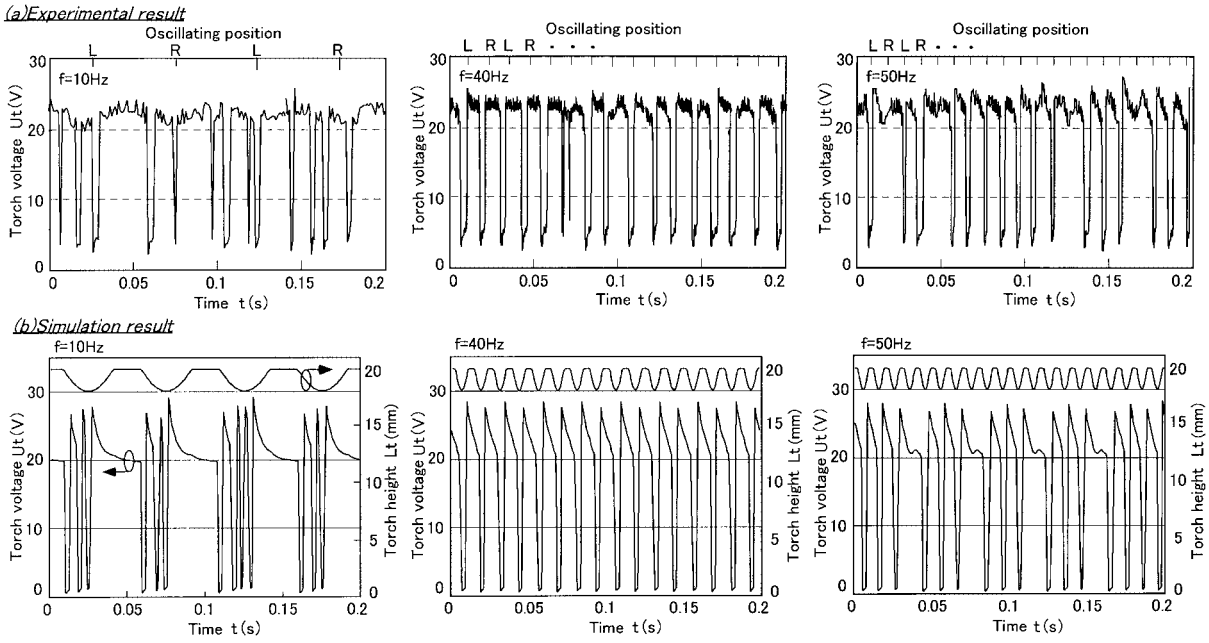

Fig. 5 Comparison between experimental result and simulation result of torch voltage history

much larger than twice the value of *f*. In this case, it is considered that the droplet grows before the wire approaches either groove wall, causing a short circuit to occur frequently, regardless of the oscillating torch position. When *f* is increased to 50 Hz or more, it becomes difficult for a short circuit to occur at either of the torch oscillation ends and the value of *Ns* decreases from twice the value of *f*. When *f* is in the range 75 to 90 Hz, the value of N_s approaches that of *f*. In this case, it is considered that a short circuit occurs once in each oscillation cycle, that is, a short circuit can occur at either oscillation end.

3.2 Optimization of oscillation frequency for arc sensor

The arc sensor is technology for seam tracking control by sensing and feeding back the changes in the welding current or torch voltage caused by oscillations of the torch. It has been widely employed under spray transfer conditions in which the welding phenomenon is stable. Under short-circuiting conditions, by contrast, it has seldom been used. With a low-frequency oscillating condition of several Hz which is commonly used, a short circuit occurs regardless of the oscillating torch position. In this case, there is the fear that any change in current/voltage due to torch oscillations would be mistaken for the variation caused by a short circuit.

By selecting a suitable oscillation frequency under high- frequency oscillation conditions, it becomes possible to limit the positions at which a short circuit occurs to the oscillation ends only. This is expected to reduce the variance in data for seam tracking control. According to the results of an analysis of arc sensor sensitivity using the frequency response method[10], the arc sensor sensitivity to both welding current signal and torch voltage signal increases in the oscillation frequency range in which the torch oscillation frequency is about half of the short-circuiting frequency without oscillations. Thus, when it comes to applying an arc sensor under short-circuiting transfer conditions, selecting the optimum oscillation frequency is an effective means of implementing highly accurate control.

4. Conclusion

As a new GAM welding process model, a model for short arc welding was developed based on the existing model for spray arc welding. In addition, by applying the new model, an analysis was conducted on the short-circuiting dynamics in a high-speed oscillating GMA process and discussed guidelines on the optimization of arc sensor properties.

This arc sensor technology has been introduced in the automatic line pipe welder MAG-II[11] for groove center tracking and oscillation width control and has proved effective in improving the quality of narrow-groove, all-position welding.

List of symbols

Symbols of spray transfer condition

A : Arc heating coefficient of wire melting, $0.22 \mathrm{mms^{-1}A^{-1}}$

B : Joule heating coefficient of wire melting, $6.3 \times 10^{-5} \mathrm{s^{-1}A^{-2}}$

E_a : Electric field intensity in arc column, $0.7 \mathrm{Vmm^{-1}}$

I : Welding current, A

J_{Le} : Joule heating weight of wire extension, $\mathrm{A^2 s}$

J_z : Joule heating weight at the location z of wire extension, $\mathrm{A^2 s}$

K_s : Slope of the U-I characteristic of power source, 0.02 Ω

L_a : Arc length, mm

L_e : Wire extension length, mm

L_s : Inductance of circuit, 2.5×10^{-4} H

L_t : Torch height ($L_e + L_a$), mm

R_a : Electric resistance of arc column, 0.03 Ω

R_c : Resistance of welding power cable, 5×10^{-3} Ω

R_e : Resistance of wire extension, Ω

r (J_z): Resistance of unit length of wire extension as a function of J_z, $9 \times 10^{-8} J_z + 3.5 \times 10^{-4}$ Ω $\mathrm{mm^{-1}}$

t : Time of simulation, s

U_a : Arc voltage, V

U_{ao} : Constant component of arc voltage, 16V

U_e : Voltage drop across wire extension, V

U_s : Equivalent output voltage of power source in the state of I = 0, V

U_t : Welding voltage ($U_a + U_e$), V

V_f : Wire feeding rate, $\mathrm{mms^{-1}}$

V_m : Wire melting rate, $\mathrm{mms^{-1}}$

τ : Time, s

Symbols of short-circuiting transfer condition

B_1 : Joule heating coefficient of wire melting at short-circuiting, $3.8 \times 10^3 \mathrm{mms^{-1}A^{-2}\,\Omega^{-1}}$

L_{em} : Droplet length, mm

L_{es} : Wire extension length of no-melting part, mm

N_s : Numbers of short-circuiting with oscillation, $\mathrm{s^{-1}}$

N_{so} : Numbers of short-circuiting without oscillation, $\mathrm{s^{-1}}$

R_m : Radius of droplet that supposed spherical shape, mm

S : Cross sectional area of wire, $\mathrm{mm^2}$

t_{ia} : Time when *i* th short-circuiting is broken, s

t_{is} : Time when *i* th short-circuiting is started, s

α : Coefficient of droplet length, 3

β : Coefficient of short-circuiting time, 200

Symbols of torch oscillation

f : Oscillating frequency in a groove, Hz

W : Oscillating width, 3mm

X : Oscillating position, mm

References

1) Lesnewich, A.: Weld. J. 37(8), 343-353(1958)
2) Halmoy, E.: Conference on Arc Physics and Weld Pool Behavior. London. 1979, p.49-57
3) Maruo, M. et al.: J.Jpn.Weld.Soc. 3(1), 191-196(1985)
4) Ushio, M. et al.: J.Jpn.Weld.Soc. 14(1), 99-107(1996)
5) Ushio, M. et al.: J.Jpn.Weld.Soc. 14(1), 108-115(1996)
6) Nomura, H. et al.: J.Jpn.Weld.Soc. 4(3), 18-23(1986)
7) Ushio, M. et al.: J.Jpn.Weld.Soc. 15(2), 272-280(1997)
8) Hirata, Y. et al.: J.Jpn.Weld.Soc. 22(2), 224-232(2004)
9) Hermans, den Ouden: Sci. Technol. Weld. Joining. 3, 135-138(1998)
10) Kodama, S. et al.: Sci. Technol. Weld. Joining. 11(1), 25-32(2006)
11) Nakamura, S. et al.: Shinnittetsu Giho. (382), 48-52(2005)